A STUDY ON STRUCTURAL DESIGN AND ANALYSIS OF COMPOSITE PROPELLER BLADE OF TURBOPROP FOR HIGH EFFICIENCY AND LIGHT WEIGHT

Changduk Kong[1], Hyunbum Park[2*], Kyungsun Lee[1], Won Choi[3]

[1]*Department of Aerospace Engineering, Chosun University, Gwangju, Rep. of Korea*
[2]*Department of Defense & Science Technology, Howon University, Gunsan, Rep. of Korea*
[3]*Research & Development Division, Korea Aerospace Industries, LTD, Sachon-City, Rep. of Korea*
**e-mail : swordship@daum.net*

Keywords: Turboprop, Propeller Blade, Skin-Spar-Foam Sandwich Structure, Structural Design

Abstract

The development of aircraft composite propeller blade is necessarily required because recently changing metal propeller to composite propeller is a global tendency due to the improvement of composite manufacture technique and good characteristics of composite materials. The complicated calculation was required at the stress analysis and the design because the aircraft propeller was in curved and twisted structure. Especially, in the case of composite propeller, the analytic method was almost impossible on account of anisotropic material properties. Therefore, the numerical analysis method must be used for the solution of the problem.

In this study, structural design and analysis of the propeller blade for turboprop aircraft, which will be a high speed transportation system for the next generation, was performed. The propeller of turboprop shall have high strength to get the thrust to fly at high speed. The high stiffness and strength carbon/epoxy composite material was used for the major structure and skin-spar-foam sandwich structural type was adopted for improvement of lightness. As a design procedure for the present study, firstly the structural design load was estimated through investigation on aerodynamic load and then flanges of spars from major bending loads and the skin from shear loads were preliminarily sized using the netting rule. In order to investigate the structural safety and stability, stress analysis was performed by finite element analysis code MSC. NASTRAN. Finally, it is investigated that designed blade have high efficiency and structural safety to analyze of aerodynamic and structural design results.

1 Introduction

Recently, the need for developing the environmental and eco-friendly aircrafts with increased fuel efficiency is being emphasized as an eco-friendly requirement in response to high oil prices. Aircrafts take up 3-5% of the world's carbon dioxide emission amount and the aircraft industry is placed at the top in the emission amount as a single industry. The amount of carbon dioxide being discharged in high altitude atmosphere is larger than that being discharged by every vehicle on the earth. Accordingly, it is necessary to develop the next-generation eco-friendly & high fuel efficiency engine technology to enhance the fuel efficiency and aerodynamic performance of aircrafts for the purpose of reducing carbon

dioxide emission amount prior to collecting and dealing with air pollution substances being discharged.

Many studies for advanced turboprop were performed. Among the previous studies, Roy H. Lange performed research about a review of advanced turboprop transport aircraft in 1986[1]. F. Farassat et al. performed the study on advanced turboprop noise prediction based on recent theoretical results in 1987[2]. This paper deals with the development of a high speed propeller noise prediction code at Langley Research Center. J. A. Liser et al. studied aeroacoustic design of a 6-bladed propeller in 1997[3]. This paper show that tip mach number reduction is a very effective way of reducing noise levels, especially when the original mach number is nearly transonic. In 2006, Quentin R. Wald performed the study on aerodynamics of propellers[4]. In this paper, the theory and the design of propellers of minimum induced loss is treated. In 1992, Takashi Yamane performed the study of aeroelastic tailoring analysis for advanced turbo propellers with composite blades[5]. In this study, the aeroelastic model of advanced composite materials is proposed. Many studies have shown that the efficiency of advanced turboprop is higher than that of the current turbofan design. After many years of study, various aerodynamic design theories were proposed. However, little research work has been carried out to propose the design method of propeller structure.

In this work, aerodynamic and structural designs of the propeller blade for an advanced turboprop aircraft, which will be used for a next generation regional commercial aircraft in Korea, are carried out. In the aerodynamic design, the parametric studies are performed to decide an optimum aerodynamic configuration having a specific HS1 series airfoil[8]. In structural design, the proposed propeller blade uses the carbon/epoxy composite skin and spar and urethane foam core sandwich type structure, so-called skin-spar-foam sandwich, is adopted. In order to confirm the initially designed propeller using the netting rule and the rule of mixture, the structural analysis including stress, eigen value and buckling analyses is performed using finite element code, MSC. NASTRAN. To finalize the proposed propeller structure design, the prototype propeller is manufactured, tested and compared with the structural analysis results.

2 Aerodynamic design

There are several design methods to size the aerodynamic blade configuration parameters such as chord length and twist angle. This work uses both the vortex theory and the blade element theory[9,13] for this purpose. The propeller blade airfoil configuration is an important factor to determine various performance parameters. In this work, the HS1 series airfoil is selected for the design purpose. Based on the regional aircraft system specification to be developed in Korea, the propeller blade design specification is briefly summarized in Table 1. The number of blades is selected as 8 blades based on previous studies[6~7].

The blade diameter is determined by the following equations[9~13].

$$D = \frac{V_t}{\pi N} \tag{1}$$

Where, V_t is blade tip speed, N is propeller rotational speed and D is propeller diameter.

The advanced ratio is defined as an important propeller design parameter in propeller design;

$$J = \frac{V_F}{ND} \tag{2}$$

Power absorbed by the blade section profile drag is estimated by the following expression;

$$P_0 = \frac{2\eta P}{3V_F}\Omega R\left(\frac{C_d}{C_l}\right)_{\alpha=0} \tag{3}$$

Where, P_0 is profile drag power, η is propeller efficiency, P is propeller power delivered from engine, Ω is propeller angular velocity, R is propeller radius, C_d is blade section drag coefficient, C_l is blade section lift coefficient and V_F is cruising speed.

The slipstream velocity can be obtained based on the momentum relationship to calculate the thrust. While the above relation is valid, it does not account for the flow distortion due to spinner, cowl and nacelle. Based on the complicated flow analysis results a simplified expression to consider the flow distortion is given by the following correction factor in the actual operation;

$$K_{(r)} = 0.7371\left(\frac{r}{E}\right)^{-0.4574} + 0.84 \tag{6}$$

$$V' = V_F(1+a)K_{(r)} \tag{7}$$

$$V_R = \sqrt{(2\pi rN)^2 + V'^2} \tag{8}$$

$$B = 1 - A \tag{9}$$

$$A = \frac{1.5958\sqrt{T/\rho}}{bDV_t} \tag{10}$$

Where, $K_{(r)}$ is correction factor, r is propeller radius, E is spinner or nacelle radius, V' is corrected inflow velocity through propeller disc, a is induced velocity factor, V_R is resultant velocity at propeller blade section, B is tip loss factor.
Finally, chord length, twisting angle and pitch angle of blade are determined by the following expression;

$$C_r = \frac{4T(r/R)}{BRb\rho V_R^2 C_l} \tag{11}$$

$$\beta = \tan^{-1}\frac{V'}{2\pi rN} \tag{12}$$

$$p = 1.50\pi R\tan\psi \tag{13}$$

Where, C_r is chord length, R is propeller tip radius, b is the number of blade, ρ is air density, β is blade angle, r is section blade radius, p is pitch and ψ is section pitch angle.
Aerodynamic design results of the propeller blade are shown in Table 2 and 3. Figure 1 shows the proposed aerodynamic configuration.

Rotation speed[RPM]	980
Velocity[m/s]	142
Thrust[kN]	10.36
Power[HP]	2229
Efficiency	0.89

Table 1. Propeller design specification

Diameter[m]	4.07
Number of Blades	8
Blade root chord[m]	0.347

Table 2. Aerodynamic design results

Section	r/R	β [degree]	Cr [mm]
A-A	0.20	65	347
B-B	0.30	63	347
C-C	0.40	59	348
D-D	0.50	55	352
E-E	0.60	50	348
F-F	0.70	46	338
G-G	0.80	41	318
H-H	0.90	39	248
I-I	1.00	35	53

Table 3. Blade angle and chord length distribution at each blade section

Aerodynamic performance including thrust, power and efficiency of the designed propeller blade are analyzed by the following expressions with thrust coefficient and power coefficient[12];

$$\frac{dC_T}{dx} = \frac{\pi^3}{4}(1-a')^2 x^3 \sigma C_y \sec^2\psi \tag{14}$$

$$\frac{dC_p}{dx} = \frac{\pi^4}{4}(1-a')^2 x^4 \sigma C_x \sec^2\psi \tag{15}$$

$$a' = \frac{\sigma C_x / a\cos\psi\sin\psi}{F - \sigma C_x / a\cos\psi\sin\psi} \tag{16}$$

$$F = \frac{2}{\pi}\cos^{-1}\exp\left(-\frac{b(1-r/R)}{2\sin\psi_T}\right) \tag{17}$$

$$C_x = C_l \sin\psi + C_d \cos\psi \tag{18}$$

$$C_y = C_l \cos\psi + C_d \sin\psi \tag{19}$$

$$\sigma = \frac{bc}{\pi D} \tag{20}$$

$$T = C_T \rho N^2 D^4 \tag{21}$$

$$P = C_P \rho N^3 D^5 \tag{22}$$

$$\eta = \frac{C_T \cdot J}{C_P} \tag{23}$$

Where, C_T is thrust coefficient, C_P is power coefficient, a' is rotational interference factor, F is Prandtl momentum loss factor, σ is solidity, T is thrust, P is power into propeller and η is propeller efficiency.

Table 4 shows aerodynamic performance calculation results. The propeller efficiency 0.878 of the proposed propeller shows better performance than other similar class existing propellers.

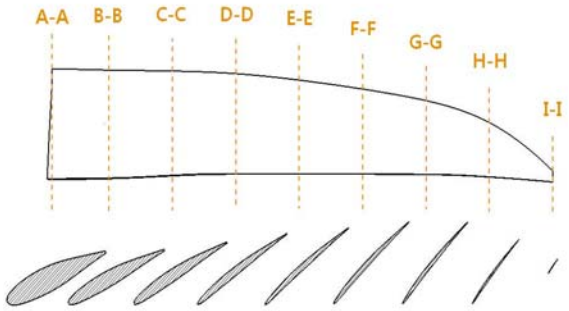

Figure 1. Aerodynamic configuration of the proposed propeller blade

J	2.12
Efficiency [%]	87.8
Thrust [N]	11563
Power [HP]	2499
β at 75% [degree]	43.9
Ct	0.239
Cp	0.567

Table 4. Aerodynamic performance calculation results

3 Structural design

Structural loads applied to the propeller blade are divided into major aerodynamic loads and subsidiary loads due to dynamic and centrifugal forces in rotation, ice, temperature and humidity effects, faults of the system, etc. in service. It is very difficult to analysis all these

loads because they are related to each other. However, because aerodynamic loads are much higher than others, they are mainly considered to avoid the design complication in preliminary structural design. Table 5 shows load cases for the blade structural design. The structural design is carried out based on the load case 3, which is the maximum load case. Figure 2 shows the bending moment diagram at design load case 1, 2, 3. Figure 3 shows the schematic blade sectional view having the skin-spar-foam sandwich structure. The proper carbon/epoxy composite fabric prepreg is selected in consideration of its mechanical property.
Preliminary structural design is initially carried out using the netting rule[14,15]. According to the netting rule, the principal load directional thickness of main spar flange can be sized by the cripple buckling strength. After the initial sizing, the structure is modified using the rule of mixture that can consider approximately 10% additional load in off-loading directions at other inclined fiber directional plies[14,15]. Therefore the initially sized 0° ply flange thickness by the netting rule is added by ±45°and 90°plies. In order to reduce the weight as well as to strengthen both the dynamic stability and the buckling strength, the sandwich structure with the urethane foam core is utilized. The main spar flange is extended to the blade tip, and its thickness is gradually decreased along the blade radius to reduce the weight. Table 6 shows the thickness distribution of the skin and spar flange along the blade radius station.

Load case 1	**Load case 2**	**Load case 3**
Cruise condition	Loiter condition	Take off condition

Table 5. Load cases for structural design

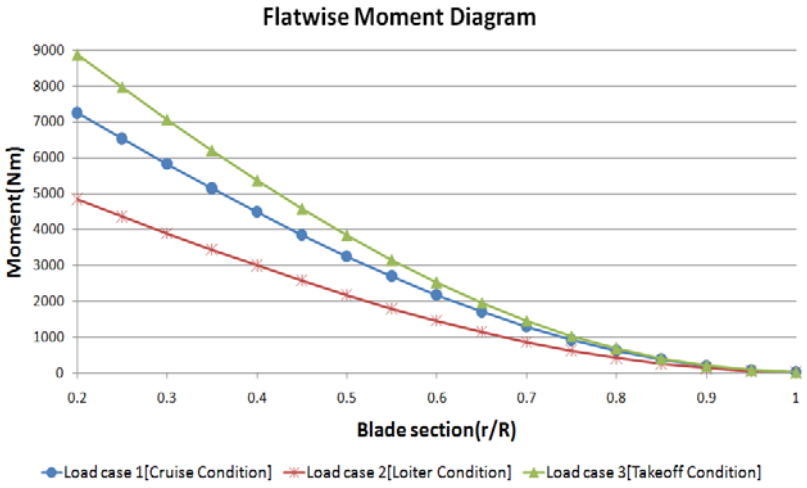

Figure 2. Bending moment diagram at design load case 1, 2, 3

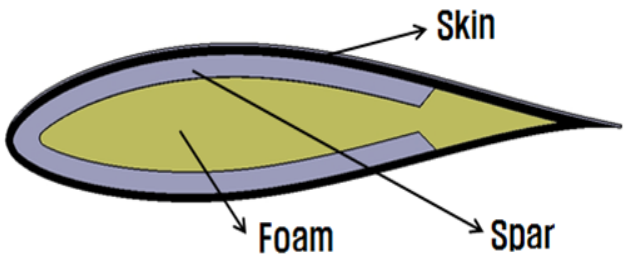

Figure 3. Schematic blade sectional view with the skin -spar-foam sandwich

Station	Spar flange	Plies
Station 1 (Root)	[(±45,04,90)10]s	140
Station 2-1	[(±45,04,90)6,±45,03]s	94
Station 2-2	[(±45,04,90)4,±45]s	60
Station 3-1	[(±45,04,90)3,±45,0]s	48
Station 3-2	[(±45,04,90)2,±45,02]s	36
Station 4-1	[(±45,04,90)2]s	28
Station 4-2	[±45,04,90]s	14
Station	**Skin**	**Plies**
Station 1~5-1	[±452,0,90,±452]s	20
Station 5-2(Tip)	[±452,0]s	10

Table 6. Thickness distribution of spar and skin along blade radius station

The structural analysis is performed using a commercial code MSC. NASTAN and the post processing program MSC. PATRAN. The element type used for the analysis is the PCOMP 4-node shell element[16]. Tsai-Wu failure criterion is used to find the structural safety. According to stress analysis results, it is found that maximum compressive stress and tensile stress on the skin are 84MPa and 90MPa, and compressive stress and tensile stress at the spar are 74MPa and 69MPa. Based on the Tsai-Wu failure criterion the minimum safety factor is 2.5, so the structural safety is confirmed. Figure 4 shows the spanwise stress distribution of the outer skin (1st ply), and Fig. 5 shows the spanwise stress distribution of the spar(23th ply) for the load case 3.

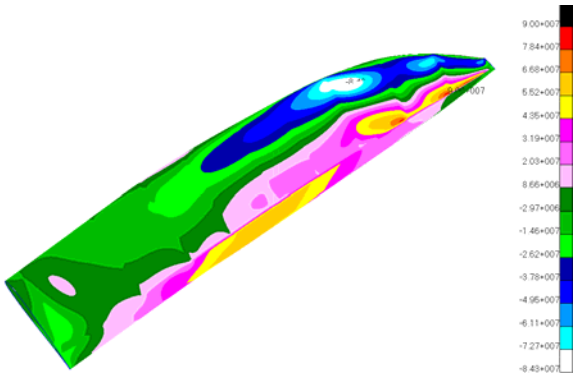

Figure 4. Spanwise stress distribution of skin (1st ply)

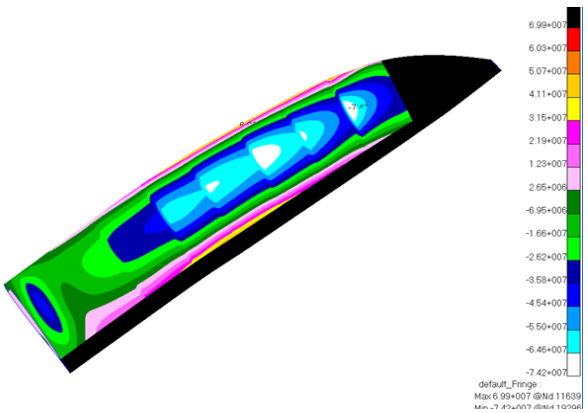

Figure 5. Spanwise stress distribution of spar (23th ply)

Dynamic effects must be substantial in a propeller blade system because of the periodic nature of its aerodynamic loading. As a result, the design process must consider the dynamic characteristics during rotation. For this purpose, the modal analysis is performed by the finite element method. Figure 6 shows Campbell diagram that the natural frequencies of both the first flap mode and the first lead lag modes are displayed whether resonances occur or not with any multiply of the rotational frequency. Resonance is a phenomenon, which occurs in a structure when the frequency of periodic loading or excitation equals or nearly equals one of the modal frequencies of the structure. Thus, as shown in Fig. 6, because there are no intersections of a radial line and a modal frequency line, any resonance between the blade and excitation loadings does not occur. Figure 7 shows the first flap mode shape in natural vibration, and Fig. 8 shows the first lead lag mode shape in natural vibration.

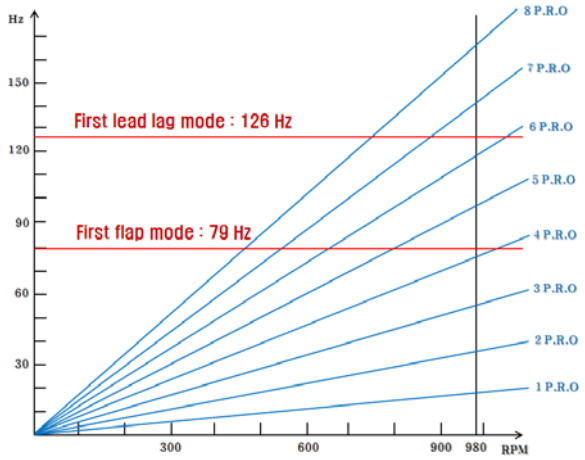

Figure 6. Campbell diagram of the designed blade

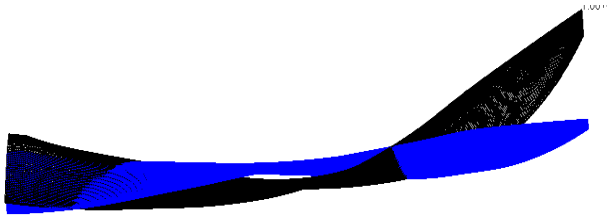

Figure 7. First flap mode shape in natural vibration

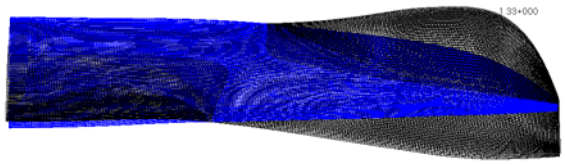

Figure 8. First lead lag mode shape in natural vibration

The buckling analysis also is done by the finite element method. The buckling analysis finite element model is the same as the static analysis model under the load case 3. Figure 9 shows the first buckling mode together with the buckling load factor. The buckling load factor means the ratio of the buckling load to the applied load. The minimum buckling load factor is found as 4.8 that is confirmed as safe from buckling.

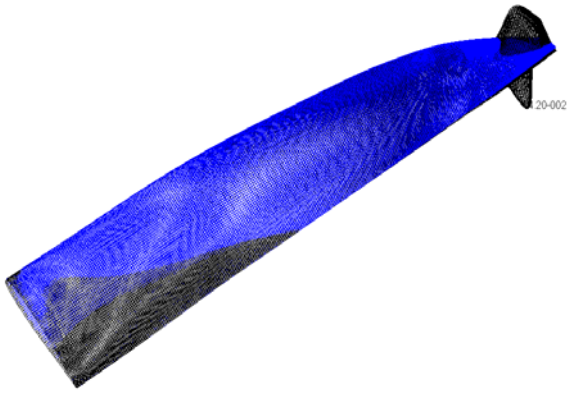

Figure 9. First buckling mode shape

4 Manufacturing and full scale structural test

The GFRP molds are made for manufacturing the prototype blade using the hand lay-up method. Surfaces of the mold are well polished and coated by a Gel coat. Then the carbon/epoxy composite fabric prepregs are laid up for skin and spar on a mold using the hand lay-up method and consolidated with a proper temperature of around 150° C and vacuum in the oven[17,18]. Figure 10 and 11 show the manufactured prototype blade.

Measurement of the blade natural frequency is performed using the impulse hammer and the stain measuring system. The dynamic strains on the blade skin due to the impact hammer are acquired by National Instruments data acquisition system. The obtained strain data are analyzed by the FFT analyzer method of LabVIEW program. Table 7 shows comparison between measured and predicted natural frequencies. As shown in the table, the predicted values are in good agreement with the measured values.

Figure 10. Complete manufactured prototype blade

Figure 11. View of prototype propeller assembly with 8 blades

Mode shape	Analysis results	Test results
First flap mode	79 Hz	85 Hz
First lead lag mode	126 Hz	135 Hz

Table 7. Comparison between measured and predicted natural frequencies

The manufactured prototype blade is set on the structural test rig and loaded at 0.9m, 1.2m and 1.5m blade stations to simulate the aerodynamics load using the three-point loading method by the hydraulic actuator, and strains and deflections of the blade are measured. The load case 3 is applied to the static structural test. Figure 12 shows load values and loading points in spanwise direction for the static strength test. Figure 13 shows the blade under loading by the three-point loading fixture. Table 8 shows comparison between predicted and measured strains and tip deflections.

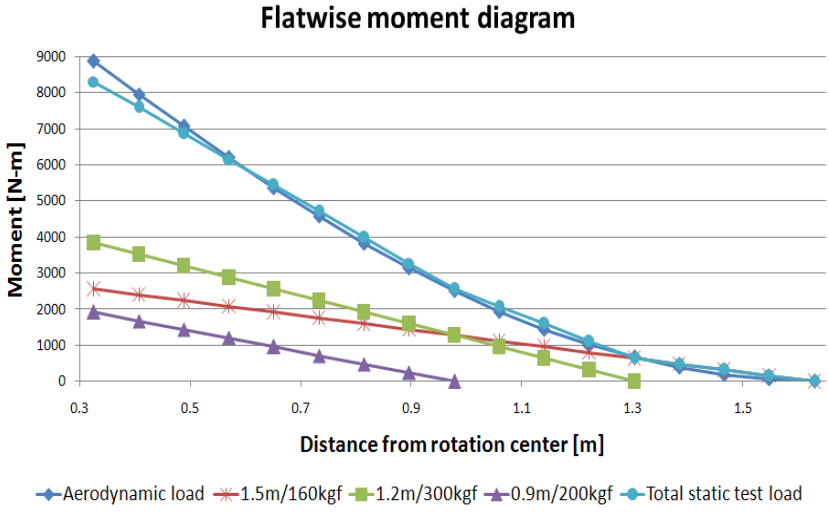

Figure 12. Static strength test loads using 3 point loading method

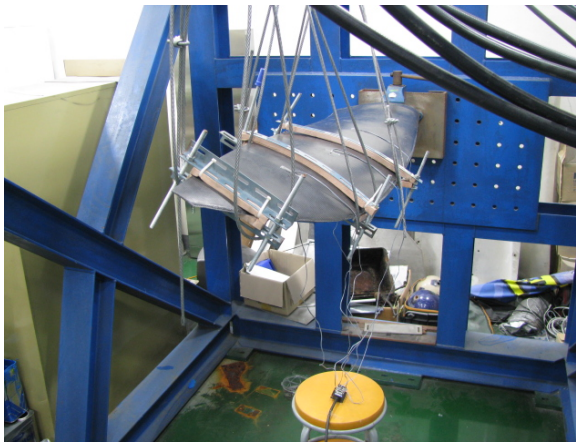

Figure 13. View of the prototype blade under loading by three-point loading fixture

Item	Analysis results	Test results	Error [%]
Tip displacement	42 mm	44 mm	4.8
Upper and lower surface strain at A point	-56μS +221μS	-67μS +236μS	16.4 6.8
Upper and lower surface strain at B point	-109μS +191μS	-129μS +211μS	18.3 10.5
Upper and lower surface strain at C point	-273μS +560μS	-297μS +583μS	8.8 4.1

Table 8. Comparison between predicted and measured strains and tip deflections

5 Conclusion

In this study, both aerodynamic and structural design of the propeller blade for an advanced regional turboprop aircraft is performed.
An optimum aerodynamic configuration of the propeller blade is proposed through the parametric studies. The propeller blade airfoil is an important factor to determine a good propeller performance. In this work the HS1 series airfoil is selected for the design purpose based on existing application examples. The proposed propeller shows better aerodynamic performance than other similar class existing propellers.
In structural design, the carbon/epoxy fabric skin-spar and urethane foam core sandwich composite structure is used to endure effectively various loads. In order to evaluate the designed structure, structural analysis is performed using the finite element method.
For manufacturing the prototype propellers, the carbon/epoxy composite fabric prepregs are laid up for skin and spar on a mold using the hand lay-up method and consolidated with a proper temperature and vacuum in the oven
The full-scale static structural test is performed under the simulated aerodynamic loads using 3 point loading method. From the experimental results, it is found that the designed blade has a good structural integrity. Furthermore, the measured results agree well with the analytical results including deflections, strains and natural frequencies.

6 Acknowledgements

The study was supported by 2011 R&D research funds from Korea Aerospace Industries, LTD. and Howon University research funds.

References

[1] Roy H. Lange, A Review of Advanced Turboprop transport aircraft, Prog. Aerospace Sci. Vol. 23, 1986, pp.151-166.
[2] F. Farassat, S. L. Padula, M.H.Dunn, Advanced turboprop noise prediction based on recent theoretical results, J. of Sound and Vibration, Vol. 119, No.1, 1987, pp53-79.
[3] J. A. Liser, D, Lonhmann, C. H. Rohardt, Aeroacoustic Design of a 6-Blades Propeller, Aerospace Science and Technology, Vol. 6, 1997, pp381-389.
[4] Quentin R. Wald The Aerodynamics of Propellers, Prog. Aerospace Sci., Vol. 42, 2006, pp.85-128.
[5] Takashi Yamane, Aeroelastic Tailoring Analysis for Advanced Turbo Propellers with Composite Blades, Computers Fluids, Vol.21, No.2, 1992, pp.235-245.
[6] Roy H. Lange, A Review of Advanced Turboprop transport aircraft, Prog. Aerospace Sci. Vol. 23, 1986, pp.151-166.
[7] J. M. Bousquet, P. Gardarein, Improvements on Computations of High Speed Propeller Unsteady Aerodynamics, Aerospace Science and Technology, Vol. 7, 2003, pp465-472.
[8] Harry S. Wainauski et al., Airfoiled Blade United State Patent, Patent Number: 4,830,574, Date of Patent: May 16 1989.
[9] Nelson, W.C., Airplane Propeller Principles, John Wiley & Sons, Inc., 1948, pp.4-34.
[10] Welch, W.A., Light plane Propeller Design, Selection, Maintenance, & Repair, Tab Books, 1979, pp.113-118.
[11] Larrabee, .E., The screw Propeller, Scientific American, Vol.243, No.1, 1980, pp.114~124.
[12] Adkins, C.N., Design of Optimum Propellers, J. of Propulsion and Power, Vol.10, No.5, Sept-Oct, 1994, pp.676~682.
[13] McCormick, B.W., Aerodynamic Aeronautics and Flight Mechanics, John Wiley & Sons, Inc., 1995, pp.291-319.
[14] C. D. Kong, H. B. Park, G. S. Lee, W. Choi, 2011. 4, A Study on Conceptual Structural Design for Composite Propeller Blade of Turboprop, Proceeding of the 2011 KSAS Spring Conference.
[15] C. D. Kong, H. B. Park, K. J. Kang, A Study on Conceptual Structural Design of Wing for a Small Scale WIG Craft Using Carbon/Epoxy and Foam Sandwich Composite Structure, Advanced Composite Materials, 2008, pp.1-16.
[16] MSC, Software, "MSC. NASTRAN 2005 Release Guide", 2005.
[17] C. Kong, T. Kim, D. Han, Y. Sugiyama, Investigation of fatigue life for a medium scale composite wind turbine blade, International Journal of Fatigue, Vol.28, 2006, pp.1382-1388.
[18] C. Kong, J. Bang, Y. Sugiyama, Structural investigation of composite wind turbine blade considering various load cases and fatigue life, ENERGY, Vol.30, 2005, pp.2101-2114.